Isotopic scaling of confinement in deuterium–tritium plasmas*

S. D. Scott,† M. C. Zarnstorff, Cris W. Barnes,[a] R. Bell, N. L. Bretz, C. Bush,[b] Z. Chang,[c] D. Ernst,[d] R. J. Fonck,[c] L. Johnson, E. Mazzucato, R. Nazikian, S. Paul, J. Schivell, E. J. Synakowski, H. Adler, M. Bell, R. Budny, E. Fredrickson, B. Grek, A. Janos, D. Johnson, D. McCune, H. Park, A. Ramsey, M. H. Redi, G. Taylor, M. Thompson, and R. Wieland

Plasma Physics Laboratory, Princeton University, Princeton, New Jersey 08543

(Received 14 November 1994; accepted 2 March 1995)

The confinement and heating of supershot plasmas are significantly enhanced with tritium beam injection relative to deuterium injection in the Tokamak Fusion Test Reactor [Plasma Phys. Controlled Fusion **26**, 11 (1984)]. The global energy confinement and local thermal transport are analyzed for deuterium and tritium fueled plasmas to quantify their dependence on the average mass of the hydrogenic ions. Radial profiles of the deuterium and tritium densities are determined from the D–T fusion neutron emission profile. The inferred scalings with average isotopic mass are quite strong, with $\tau_E \propto \langle A \rangle^{0.85\pm0.20}$, $\tau_E^{\text{thermal}} \propto \langle A \rangle^{0.89\pm0.20}$, $\chi_i^{\text{tot}} \propto \langle A \rangle^{-2.6\pm0.5}$, and $D_e \propto \langle A \rangle^{-1.4\pm0.2}$ at fixed P_{inj}. For fixed local plasma parameters $\chi_i^{\text{tot}} \propto \langle A \rangle^{-1.8\pm0.4}$ is obtained. The quoted 2σ uncertainties include contributions from both diagnostic errors and shot irreproducibility, and are conservatively constructed to attribute the entire scatter in the regressed parameters to uncertainties in the exponent on plasma mass. © *1995 American Institute of Physics.*

I. INTRODUCTION

The variation of energy and particle confinement with plasma composition in tokamaks represents a significant uncertainty for estimating the energy confinement time in ignited reactors. Previous experiments in many tokamaks have compared confinement and transport in hydrogen, deuterium, and helium plasmas with a variety of heating methods and in a number of different confinement regimes. A common observation is that both energy and particle confinement are better in deuterium than in hydrogen plasmas, although the magnitude of the improvement varies considerably among the plasma regimes and even among different tokamaks operating in nominally the same plasma regime. Regression analyses of confinement results from many tokamaks,[1] including the International Thermonuclear Experimental Reactor (ITER) confinement scalings,[2,3] have characterized the dependence as a simple power law, with $\tau_E \propto A^{0.4-0.5}$. The overall trend is clearly favorable for tokamak ignition, since it projects to better energy confinement in deuterium–tritium plasmas relative to the hydrogen and deuterium plasmas that have been studied previously. However, the observed variation of the strength of the isotope improvement among the different plasma regimes is not well understood experimentally or theoretically, and measurements of isotope variation of *local* heat transport coefficients, separated for ions and electrons, are very limited. The favorable isotopic scaling of confinement is opposite to what is expected from simple neoclassical or gyro-Bohm theoretical models of plasma transport, although recent models are showing increasing sophistication in their nonlinear treatment of experimental conditions, including the presence of multiple ion species and nonthermal ions.[4,5]

In this paper we analyze the variation of energy, particle, and momentum transport with isotopic mass in the Tokamak Fusion Test Reactor (TFTR)[6] for deuterium (D) and deuterium–tritium (D–T) plasmas.[7] The plasmas studied here are in the enhanced confinement supershot regime,[8] characterized by high ion temperature (~30 keV), high fusion reactivity, confinement enhancement of up to three times low-mode (L-mode) scalings, and peaked density profiles. Local profile measurements of electron density, ion and electron temperature, toroidal rotation speed, and plasma isotopic composition are used to deduce the isotopic dependence of local transport coefficients. Ion–electron equipartition power is minimized by virtue of high electron temperature and modest plasma density, which allows the ion and electron transport to be investigated separately. Local ion heat transport is observed to be a factor of 2 lower in the D–T plasmas than in the D plasmas, despite only relatively modest changes in plasma composition. This result is corroborated by measurements of comparable reductions in local momentum transport, which has been found to correlate with ion heat transport in other experiments.[9,10] Somewhat smaller reductions in electron particle and heat transport coefficients are also observed. The observation of such a strongly favorable isotope dependence of *any* transport coefficient poses a useful benchmark for theoretical transport models. In addition, it suggests the possibility of significantly higher-energy confinement projections for D–T–ITER plasmas, since ions are often found to be the dominant energy loss channel for supershot, L-mode, and high-mode (H-mode) plasmas.[11]

This study follows measurements of higher-energy con-

*Paper 2IA1, Bull. Am. Phys. Soc. **39**, 1544 (1994).
†Invited speaker.
[a]Permanent address: Los Alamos National Laboratory, Los Alamos, New Mexico 87545.
[b]Permanent address: Oak Ridge National Laboratory, Oak Ridge, Tennessee 37831.
[c]Permanent address: University of Wisconsin, Madison, Wisconsin 53706.
[d]Permanent address: Massachusetts Institute of Technology, Cambridge, Massachusetts 02139.

finement time and higher ion temperature in the first TFTR campaign in D–T plasmas at high heating power.[12] Supershot plasmas heated by roughly equal amounts of tritium and deuterium beams obtained 20%–25% higher central ion temperature and up to 22% higher total stored energy compared to plasmas heated with deuterium beams alone. These results indicated better ion energy confinement in the D–T plasmas;[12,13] however, the experimental conditions were optimized for maximizing fusion power rather than local transport studies. The plasmas explored only a limited range in tritium concentration, and typically experienced a decline in confinement performance after ~0.5 s, due to low m/n magnetohydrodynamic (MHD) activity or hydrogen influx from the limiter surface.

Following a review of previous studies of isotope scaling in various regimes, we present an analysis of the isotopic mass scaling of the global energy confinement time of D–T plasmas, followed by an analysis of the plasma profiles and heating, and the inferred scaling of the local transport.

II. REVIEW OF ISOTOPIC SCALING IN OTHER REGIMES

Favorable isotope scaling of τ_E is a very common observation in Ohmic plasmas, both at low and high density,[1] very roughly characterized as $\tau_E^{\mathrm{OH}} \propto A_i^{0.5}$. A stronger isotope dependence has been observed in low-density, L-mode DIII-D plasmas with electron cyclotron heating,[14] $\tau_E \propto A_i^{0.74}$. Since in these regimes radial heat flow is dominated by electrons, the favorable isotopic scaling of global τ_E is strong evidence for a favorable isotopic scaling of electron energy confinement. Favorable isotopic scaling of global τ_E has also been observed in the high-density saturated Ohmic confinement (SOC) regime. It has been pointed out that this may suggest favorable isotope scaling of τ_{Ei}, since ion energy losses are significant there.[15] However, this result seems less conclusively demonstrated than the isotope scaling of electron energy confinement.

The isotope scaling of ion energy transport is perhaps more easily explored in the beam-heated L-mode regime, for which measured ion temperature profiles are available, and for which ions often dominate the radial power flow.[16,17] As discussed below, τ_E appears to have a weaker isotope scaling in the L-mode regime than in the Ohmic regime, with little evidence for favorable isotope scaling of τ_{Ei}.

DIII-D has obtained the weakest isotope effect in L-mode plasmas, seeing essentially no difference in global τ_E between hydrogen and deuterium plasmas heated with hydrogen beams.[18,19] ASDEX observed a modest isotope scaling of global energy confinement in beam-heated L-mode plasmas, $\tau_E^{\mathrm{L\,mode}} \propto A_i^{0.34\pm0.02}$.[20,1] The electron stored energy showed a positive isotope effect, $W_e \propto A_i^{0.24}$. Two-fluid power balance analysis to determine the isotope effect on ion energy confinement is not available. JET observed a 25%±5% increase between relatively pure hydrogen and deuterium L-mode plasmas[21] under nominally matched conditions and similar beam deposition profiles (140 keV $H^0 \rightarrow H^+$ vs 100 keV $D^0 \rightarrow D^+$; $I_p = 3.1$ MA, $P_b \approx 6$ MW). Part of this difference was due to a larger beam stored energy in the deuterium plasmas, so the inferred improvement in τ_E^{th} was only 15%±10%. If represented as a power-law scaling, the observed variation in JET confinement times can be represented roughly as $\tau_E^{\mathrm{tot}} \propto \langle A \rangle^{0.32\pm0.06}$ and $\tau_E^{\mathrm{th}} \propto \langle A \rangle^{0.20\pm0.12}$. Central electron temperatures were consistently larger in the deuterium plasmas, along with longer particle confinement times. Ion temperature profile measurements were not available for the hydrogen plasmas, so it was not possible to determine whether ions or electrons or both experienced an isotope effect.

TFTR has compared hydrogen to deuterium L-mode transport in plasmas having carefully matched conditions ($R = 2.45$ m, $a = 0.80$ m, $I_p = 1.4$ MA, $P_b \leq 8$ MW, and $\bar{n}_{e19} = 2.9-4.4$). These experiments used deuterium beams exclusively, comparing $D^0 \rightarrow H^+$ versus $D^0 \rightarrow D^+$, and consequently explored a limited range of isotopic mix, ranging from about 10% hydrogen to 65% hydrogen. Similar to the JET experience, the deuterium plasmas realized 15%–20% larger total stored energy. Approximately half of the improvement was due to differences in the beam stored energy, and the increase in τ_E^{th} determined from temperature profile measurements was only ~10%. Taking into account the smaller range of isotopic mix, these results imply $\tau_E^{\mathrm{tot}} \propto \langle A \rangle^{0.41-0.53}$ and $\tau_E^{\mathrm{th}} \propto \langle A \rangle^{-0.28}$. As in the JET experiments, higher central electron temperatures and electron energy densities were achieved in the deuterium plasmas. Two-fluid transport analysis showed a modest improvement in core electron energy confinement, but no appreciable improvement in ion energy or momentum confinement.

Considerable variability in the improvement in global τ_E between hydrogen and deuterium H-mode plasmas has been observed, ranging from a null result in JAERI Fusion Torus 2 Modified JFT-2M,[22] to a factor-of-2 improvement in DIII-D[18] and ASDEX.[1] Measurements of the isotope scaling of *local* transport coefficients in H-mode plasmas have not been reported. The situation in H-mode plasmas is complicated by the significant contribution of the edge pedestal to total stored energy and τ_E, which, in turn, is affected by differing behavior of edge localized modes in hydrogen and deuterium plasmas.

Of possibly greater relevance to the TFTR supershot isotope scaling experiments are previous results reported by Tokamak Experiment for Technically Oriented Research (TEXTOR), which observed a strong isotope scaling of energy confinement in its I-mode regime[23] of plasma operation. Approximately 25% more *thermal* stored energy was obtained during 1.7 MW deuterium beam injection than during hydrogen beam injection of the same power, a larger improvement than the typical L-mode increment in τ_E^{th}. The I-mode regime has several characteristics in common with the TFTR supershot regime, including $T_i > T_e$, a peaked electron density profile, and the requirement of at least some codirected neutral beam power. This suggests that the same physics mechanisms may be controlling the strong isotope scaling in both regimes.

III. PLASMA CONDITIONS AND GLOBAL SCALING

The plasmas considered here are fueled by either pure deuterium or pure tritium neutral beam injection (NBI) to

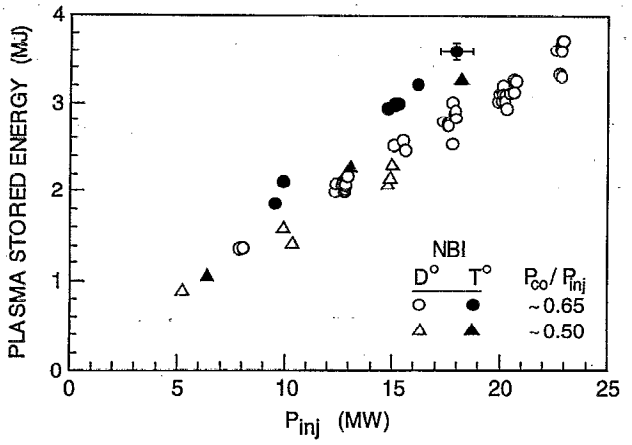

FIG. 1. Variation of stored energy with injected power for deuterium (D) and tritium (T) fueled supershots, with $I_P=1.6$ MA and either balanced injection ($P_{co}/P_{inj}=0.5$) or slightly coinjection ($P_{co}/P_{inj}=0.65$).

maximize the isotopic effects, and to minimize contributions from fusion-produced α particles to the plasma stored energy or heating. The plasmas studied have $I_P=1.6$ MA, $R=2.52$ m, $B_T=4.8$ T, and include power scans up to $P_{inj}\sim 23$ MW of either nearly balanced co- and countertangential NBI or cotangential only NBI. All plasmas discussed achieve transport (particle and energy) equilibrium within the 1.4 s heating pulse, with no significant confinement degradation or MHD instabilities. During the period of auxiliary heating, q_ψ changes less than 0.2 throughout the region $r/a\leqslant 0.9$. Figure 1 shows the variation of the plasma stored energy W_{tot} (from magnetic measurements) with P_{inj} for either D-NBI or T-NBI, for both near-balanced injection and unbalanced injection. At high beam power, W_{tot} is consistently enhanced by ~25% for T-NBI plasmas relative to comparable D-NBI plasmas. As previously observed in the supershot regime, energy confinement is optimized in both T-NBI and D-NBI plasmas with slightly more co- than counterinjected power; τ_E is consistently about 10% higher at $P_{co}/P_{inj}\sim 0.65$ than at $P_{co}/P_{inj}\sim 0.50$. As desired, fusion-generated alpha populations in these plasmas represent only very small perturbations to the heating and stored energy. Even for the highest-power T-NBI shots, the classically expected α-particle stored energy is less than 2.5% of W_{tot} and the associated heating power is less than 3% of applied heating power. Near the plasma center ($r/a\leqslant 0.25$), where the α birth rate is strongly peaked, heating by α particles still represents less than 10% of the total power delivered to electrons, and less than 2% of the total power delivered to ions.

For the T-NBI plasmas shown in Fig. 1, the limiter hydrogenic recycling influx, as measured by $H_\alpha/D_\alpha/T_\alpha$ spectroscopy,[24] is dominated by deuterium, with only ~2% due to tritium and ~18% due to hydrogen. From measurements of the D–T neutron emission profile (Sec. VI), the tritium fraction of the thermal hydrogenic ions within $r/a=0.5$ is calculated to be ~60% for the highest power T-NBI plasma. Thus, a significant portion of the central thermal hydrogenic ion density is due to particles originating from the limiter. For the low-power T-NBI plasmas, the thermal tritium fraction is calculated to be ~28%, explaining its smaller confinement enhancement above similar D-NBI plasmas.

The fraction of P_{inj} radiated in these plasmas is ~30% for $P_{inj}\sim 5$ MW, decreasing to ~25% at high power. The radiated power fraction is comparable within measurement accuracy in the D-NBI and T-NBI plasmas, being lower by ~3% during T-NBI, resulting in slightly higher limiter power loading. The radiation is emitted near the plasma edge, during both D-NBI and T-NBI, as measured by bolometer arrays, and is negligible in the plasma core. When comparing matched D-NBI and T-NBI plasmas at a given P_{inj}, the edge hydrogenic recycling remains constant to within 5%–10%. The edge CII emission is often up to 20% higher in T-NBI plasmas. In D-NBI plasmas, higher edge CII emission correlates with *lower* confinement. Thus, neither radiated power nor edge recycling appears to play a significant role in the observed confinement improvement with T-NBI, in contrast to H/D isotopic comparisons on ASDEX.[1]

IV. PROFILE ANALYSIS

To understand the origin of the improved confinement with T-NBI, these plasmas are analyzed using the steady-state transport analysis code SNAP[25] and the time-dependent code TRANSP,[26] using experimentally measured temperature and density profiles. Here $T_e(r,t)$ is measured by electron cyclotron spectroscopy (ECE) and Thomson scattering, $T_i(r,t)$ and toroidal rotation velocity $v_\phi(r,t)$ are measured by carbon charge-exchange recombination spectroscopy (CHERS), and $n_e(r,t)$ is measured by a ten-channel infrared interferometer array. The ion depletion is calculated using tangential visible-bremsstrahlung measurements for Z_{eff} and x-ray spectroscopic measurements of metallic concentrations.

Due to the change in the beam–neutral velocities between D-NBI and T-NBI at fixed acceleration voltage, the CHERS measurements suffer a systematic offset in the apparent T_i and v_ϕ due to the variation of the carbon charge-exchange emission cross section, with the relative velocity between the hydrogenic neutral and the C^{6+} ion.[27,28] This effect has been verified by comparing CHERS measurements of the same D–T plasma using either D or T doping beams, and by comparing measurements of spinning plasmas using co- and counterdirected neutral beams, as a function of plasma rotation velocity. The offsets are found to be in good agreement with simulations of the charge exchange spectral line shape and position based on a published fit to experimental and theoretical capture cross sections.[29] The T_i and v_ϕ measurements used for this analysis are corrected for this effect, using beam deposition calculations in SNAP and TRANSP to calculate the fast neutral energy spectrum in the plasma frame. The correction to v_ϕ reaches $\sim 2.3\times 10^5$ m/s for $T_i\sim 30$ keV. The correction to T_i is ~10% at the plasma center where $T_i\approx 30$ keV, but decreases rapidly at lower temperatures, and is $\leqslant 5\%$ for $T_i\leqslant 20$ keV. The difference between the measured carbon–ion temperature and the deuterium temperature due to preferential beam power coupling to impurities is calculated to be less than 1.5 keV for the high P_{inj} plasmas.

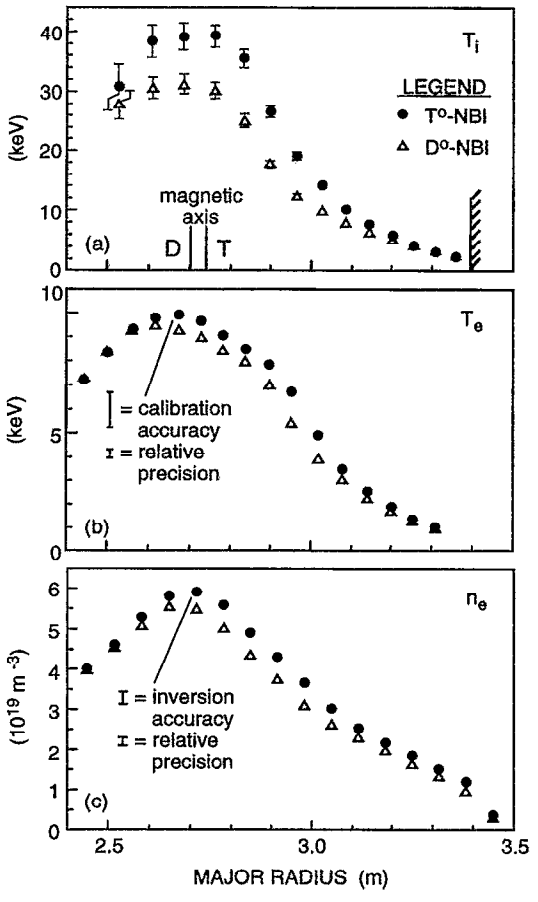

FIG. 2. Comparison of measured profiles of ion and electron temperatures and electron density in deuterium and tritium plasmas, for $I_P = 1.6$ MA and $P_B = 18$ MW. Note that the Shafronov shift of the profiles has changed due to the change in stored energy between D-NBI and T-NBI.

Comparing carefully matched sets of D-NBI and T-NBI plasmas, for which all the externally controlled discharge parameters and the target plasma are nominally identical, a consistent and clear improvement in plasma performance is observed with T-NBI. As shown in Fig. 2, T-NBI plasmas typically have a ~25% higher central ion temperature and a 5%–10% higher central electron temperature. The central Z_{eff} for the T-NBI plasma is 2.3, while the D-NBI plasma has $Z_{\text{eff}}=2.5$, a difference comparable to the shot-to-shot variation observed in similarly prepared deuterium plasmas. The measured plasma density profiles have the same shape, but the T-NBI plasma density is ~10% higher. Within the cluster of other D-NBI plasmas with $P_{\text{inj}}=18$ MW in Fig. 1 are plasmas with the same Z_{eff} or n_e profile as the T-NBI plasma. Due to their larger W_{tot}, the T-NBI profiles show a larger Shafranov shift than the D-NBI profiles. For high P_{inj}, 65%–80% of the increase in W_{tot} is accounted for by the increase in the thermal ion and electron energy content, with the rest due to the expected classical increase in the circulating beam particles and the small contribution from α particles.

Many of the systematic diagnostic uncertainties are common to measurements in D-NBI and T-NBI discharges, because the plasma conditions are quite similar. Thus, the accuracy with which an isotope dependence can be determined for many transport parameters is limited primarily by statistical diagnostic errors and the shot-to-shot drift of diagnostic calibrations, excluding most systematic errors, except a few that potentially differ between D-NBI and T-NBI, such as the beam power calibration and the ion temperature measurement. Figure 2 shows the total diagnostic uncertainty and relative precision for the ECE $T_e(R)$ measurement (±8% and ±2%, respectively), and for the interferometer $n_e(R)$ measurement (±2% and ±1%). A ±5% relative uncertainty is estimated for the beam power calibration between D-NBI and T-NBI. The uncertainty in total stored energy determined from diamagnetic and equilibrium-field measurements is approximately ±0.07 MJ, while the relative precision is about a factor of 2 smaller, ±0.03 MJ. Uncertainty in the ion-temperature measurement includes a small contribution from the uncertainty in modeling the energy dependence of the charge-exchange cross section (2%), plus a dominant term from counting and background-subtraction statistics. The uncertainty in measured v_ϕ (which affects the inference of momentum transport, but which has little effect on other transport coefficients) includes a statistical component, but not the modeling uncertainty, which has not yet been determined.

To calculate error bars on the computed diffusivities, an ensemble of 100 transport analyses was performed for the two discharges shown in Fig. 1, and approximately 30 transport analyses for other discharges in the dataset, simultaneously varying the measured profiles an other input data within their ranges of uncertainty. Quoted uncertainties in various power-law fits to the isotopic mass scaling (e.g., $\chi_i^{\text{tot}} \propto \langle A\rangle^{-2.6\pm0.5}$) represent the 2σ width of a frequency plot of $\{\log(\chi_i^{\text{tot}}) - \log[\chi_i^{\text{tot}}(\text{fit})]\}/\log\langle A\rangle$, which effectively attributes the entire scatter of the measured χ_i^{tot} values in the dataset about the power-law expression $\chi_i^{\text{tot}}(\text{fit})$ to uncertainties in the exponent on plasma mass.

V. TRANSPORT ANALYSIS

The SNAP and TRANSP model the deposition of the injected beam neutral atoms, and the subsequent slowing down and losses of the fast ions. These codes calculate the beam deposition profile by tracking beam neutrals along their linear trajectories until they are born as fast ions through ionization or charge exchange. The resulting beam-ion population is calculated, assuming classical beam-ion thermalization, through solution of the Fokker Planck equation (SNAP) or guiding-center Monte Carlo orbit calculations (TRANSP). To assess the consistency of the diagnostics and kinetic modeling, we compare the magnetically measured energy content W_{mag} with the kinetic stored energy W_{kin} calculated from the measured thermal temperature and density profiles and the modeled beam ion distribution function. Using the ECE T_e measurements, W_{kin} is within 10% of W_{mag}, which is within their combined uncertainties. The Thomson scattering T_e measurement has a lower central T_e and a broader profile than the ECE measurement, resulting in an increased calculated W_{kin}. The resulting W_{kin} is consistently higher than W_{mag} by ~10% at high P_{inj} and 20% high at

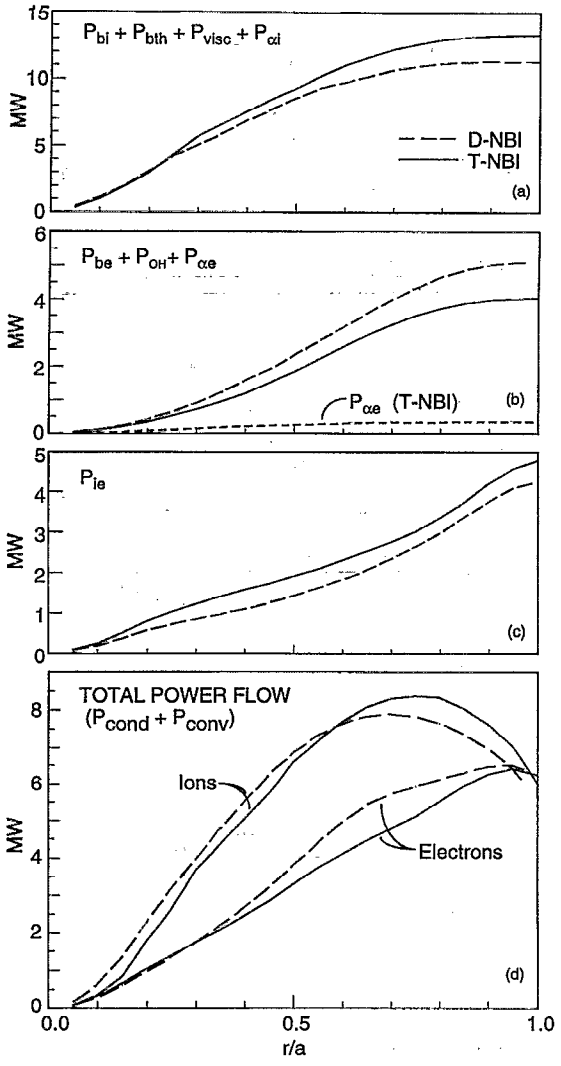

FIG. 3. TRANSP-calculated profiles of plasma heating for the D- and T-NBI plasmas of Fig. 2. (a) Direct power deposition to thermal ions; (b) direct power deposition to thermal electrons; (c) equilibration power from ions to electrons; (d) net power flow through ions and electrons.

P_{inj}=5 MW. Because of this higher level of disagreement, only results based on ECE T_e measurements will be discussed here.

There are a number of small, classically expected differences between T- and D-neutral beam heating that are included in the analysis. The lower beam particle velocity of T-NBI broadens the power deposition profile slightly, reducing beam power deposition on axis by 5%–10% during T-NBI relative to D-NBI at high power (P_{inj}=18 MW). The lower beam velocity during T-NBI also increases the fraction of beam power collisionally coupled to thermal ions, and correspondingly reduces the fraction to thermal electrons. As shown in Fig. 3, these effects roughly cancel for ion heating in the core, while they both penalize core electron heating, which remains smaller during T-NBI, despite the additional heating by α particles. The higher ion temperatures realized with T-NBI increases ion–electron equilibration power, so the radial power flow through thermal ions ($P^i_{flow} \equiv P_{bi} + P_{bth} + P_{visc} + P_{\alpha i} - P_{ie} - \dot{W}_i$) is somewhat less during T-NBI than during D-NBI over most of the plasma cross section. At the time shown, the time rate of change of ion and electron stored energy is small compared to the corresponding radial power flow, 3.5% for ions and 9% for electrons at the plasma half-radius. Most of the radial power flow is carried by thermal ions. The accuracy of the beam deposition modeling has been evaluated by comparing the rate of rise of central electron density at the initiation of beam injection with the electron source rate calculated by TRANSP. The calculated and measured central particle source rates due to beam injection agree to better than 10% for both the D-NBI and T-NBI plasmas.

As previously observed in supershots,[30] energy transport near the magnetic axis is dominated by $\frac{3}{2}\Gamma T$ convective losses, particularly for the higher-temperature T-NBI plasmas. At $r \sim a/2$, the convective losses are small, and the transport is dominated by conduction. In order to treat the transport in both regions and to avoid prescribing a particular convective multiplier, the local transport is characterized here by *total* effective diffusivities,

$$Q_{i,e} \equiv -\chi^{tot}_{i,e} n_{i,e} \nabla T_{i,e},$$

$$\Gamma_e \equiv -D_e \nabla n_e,$$

where Q_i and Q_e are the total ion and electron radial energy fluxes, Γ_e is the electron radial particle flux, and $n_i = \Sigma_j n_j$ is the total thermal ion density.

VI. ISOTOPIC CONTENT

The isotopic content of the plasma must be measured in order to understand any transport variations observed. In the D-NBI plasmas, the absence of a significant tritium density is confirmed by the measured low level of D–T fusion neutron emission. In the T-NBI plasmas, the deuterium influx from the limiter surface is a significant source of particles, and leads to a significant deuterium density n_d throughout the plasma. Since there are no deuterium beams during T-NBI, the local D–T neutron emission rate arises solely from interactions between the wall-evolved deuterons and thermal or beam tritons. The local D–T neutron emission profile is determined by Abel inverting measurements by a ten-channel collimated neutron-detector array. The radial profile of thermal n_d is constructed to reproduce the measured D–T neutron emissivity, using calculated plasma D–T reactivity profiles for beam–thermal and thermal–thermal reactions from the TRANSP code. The hydrogen density, n_h, is determined by assuming that $n_h(r)$ and $n_d(r)$ have the same profile shape and are in the same ratio as the measured edge H_α and D_α intensities, since the only source of hydrogen and deuterium is edge recycling in T-NBI plasmas. Finally, the tritium thermal density is calculated by subtracting n_h and n_d from the total hydrogenic ion density, which is the measured local electron density minus impurity and beam-ion dilution. The central n_d is found to rise slowly during the equilibrium phase of the NBI pulse in approximately fixed ratio to the edge D_α emission.

Typical inferred equilibrium n_d and n_t profiles are shown in Fig. 4. Note that the n_d profile is relatively flat,

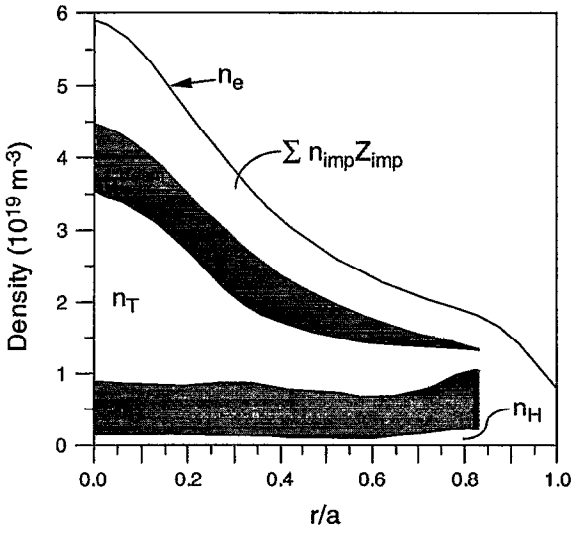

FIG. 4. The hydrogen, deuterium, tritium, tritium beam, and electron densities in the T-NBI plasma of Fig. 2. Each region represents the density of the indicated species. The deuterium and tritium densities are determined from the measured D–T neutron emission profile and the plasma reactivity profiles calculated by TRANSP.

indicating the absence of any significant deuterium particle pinch in these cases. The central deuterium density during T-NBI is inferred with an estimated accuracy of ±20%, limited by the 7% accuracy of the multichannel neutron collimator diagnostic and ~15% modeling uncertainties. The implied absence of a significant ion particle pinch in these plasmas is similar to the results of the tritium gas puffing experiments.[31]

VII. ENERGY AND PARTICLE TRANSPORT

Figure 5 compares the inferred local diffusivities for the matched T-NBI and D-NBI plasmas of Fig. 2. The power balance analysis consistently indicates that the higher T_i gradient observed during T-NBI, in the presence of reduced net ion heating, is due to a reduction of the ion thermal diffusivity χ_i^{tot} by a factor of ~2 for $r/a \leq 0.5$. The lack of substantial change in the density gradient, despite the broader beam deposition profile with T-NBI, is interpreted as a drop in the core electron particle diffusivity D_e by ~20%. The electron thermal diffusivity χ_e^{tot} is often observed to be higher in the core with T-NBI, but can be lower near $r/a \sim 0.5$ by ~10%. As shown in Fig. 6, this strong reduction in χ_i^{tot} and weak reduction in χ_e^{tot} is clearly present throughout the dataset, except at low power, where the fractional tritium density is small.

The isotopic mix of these plasmas has been characterized by the average mass of the central thermal hydrogenic ions, $\langle A \rangle$, within $r/a = 0.5$, since this radius contains more than three-fourths of the thermal stored energy. This volume-averaged mass is approximately equal to the local average hydrogenic mass at $r = a/3$. The plasmas studied range from $\langle A \rangle = 1.9$ (D-NBI), to $\langle A \rangle = 2.1$ at 6.4 MW T-NBI, to $\langle A \rangle = 2.5$ at 18 MW T-NBI. Thus, the core of the 18 MW T-NBI plasmas has the same average isotopic mix as expected for ITER and future reactors. The observed variations of the

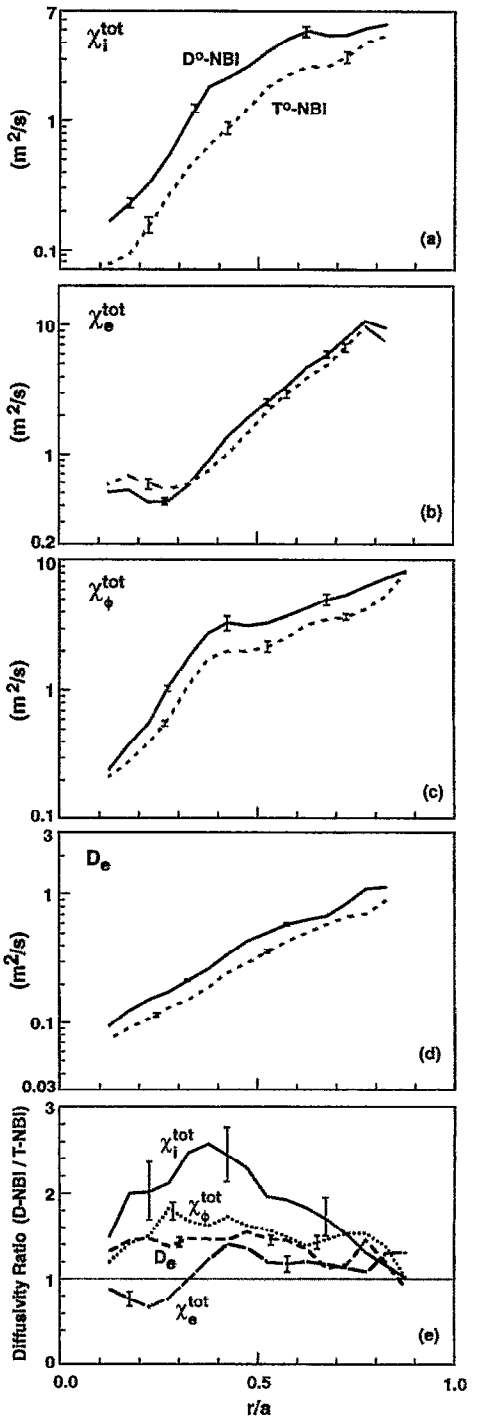

FIG. 5. Comparison of the transport coefficients inferred between the D-NBI and T-NBI plasmas of Fig. 2. (a) χ_i^{tot}; (b) χ_e^{tot}; (c) χ_ϕ^{tot}; (d) D_e; and (e) ratio of the D-NBI and T-NBI coefficients. The data for χ_ϕ^{tot} are taken from a pair of D-NBI and T-NBI plasmas with pure codirected beam injection at $P_{inj} = 12.5$ MW under otherwise comparable conditions.

plasma parameters and transport coefficients for the T-NBI plasmas relative to the matched D-NBI plasmas can be expressed as a power-law dependence on $\langle A \rangle$. Strong dependencies on $\langle A \rangle$ are inferred, due to the strong variations observed and the moderate range of $\langle A \rangle$ studied. The total

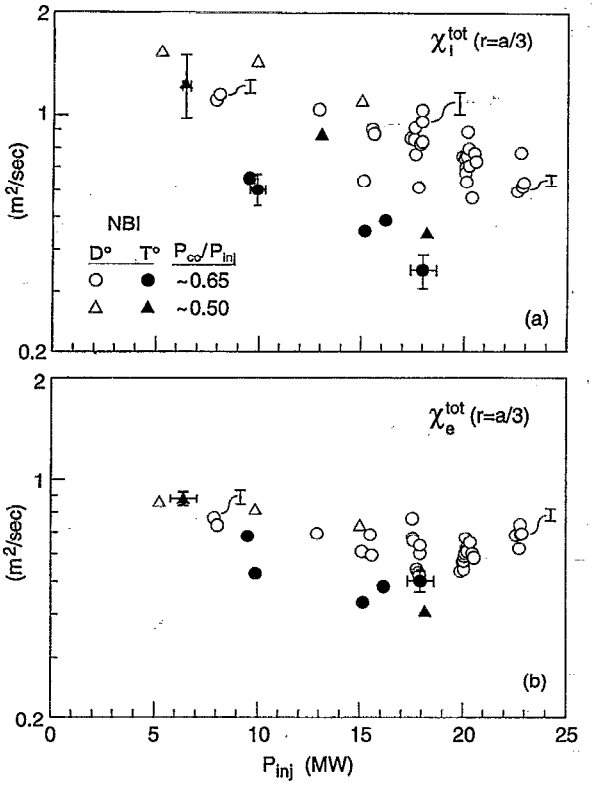

FIG. 6. Variation of (a) χ_i^{tot} and (b) χ_e^{tot} with P_{inj} at $r/a=\frac{1}{3}$.

stored energy analyzed in this fashion scales as $W_{tot} \propto \langle A \rangle^{0.85\pm0.20}$ and the thermal stored energy scales as $W_{thermal} \propto \langle A \rangle^{0.89\pm0.20}$. Including the fraction of beam power in the codirection (P_{co}/P_{inj}) as a regression variable, does not change the inferred isotope variation of W_{tot} beyond the ±0.20 uncertainty.

In the plasma core, $r/a \sim \frac{1}{3}$, $\chi_i^{tot} \propto \langle A \rangle^{-2.6\pm0.5}$, $\chi_e^{tot} \propto \langle A \rangle^{-1.2\pm0.4}$, and $D_e \propto \langle A \rangle^{-1.4\pm0.2}$ for fixed P_{inj}. Thomson scattering indicates a smaller increase in electron temperature between D-NBI and T-NBI plasmas than does ECE, and at the present time it is not possible to clearly demonstrate a favorable isotope scaling of χ_e^{tot} based on the Thomson data.

VIII. MOMENTUM TRANSPORT

The isotopic scaling of the momentum transport is measured in a companion scan of the applied neutral–beam torque using unidirectional co-only injection. As shown in Fig. 7, the central angular momentum density is ~50% higher for T-NBI than for D-NBI at a fixed injected torque, indicating improved momentum confinement in the D–T plasma. Much of the increase in momentum density is due to the higher tritium mass. The momentum transport is analyzed in terms of an angular momentum diffusivity,

$$\Gamma_\phi \equiv -\chi_\phi^{tot} R n_i m_i \nabla v_\phi,$$

where Γ_ϕ is the radial flux of angular momentum. Figure 5 compares the inferred χ_ϕ^{tot} profile for T-NBI and D-NBI plasmas at $P_{inj}=12.5$ MW in the torque scan. At this power, χ_ϕ^{tot} was reduced by ~30%–40% in the T-NBI plasma relative to

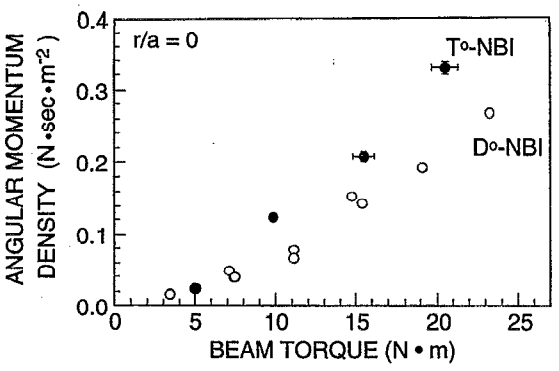

FIG. 7. Increase in central angular momentum density with increasing applied beam torque with unidirectional co-only injection for both T-NBI and D-NBI.

the D-NBI plasma, similar to the reduction of χ_i^{tot} found for near-balanced plasmas at this power level. This result is consistent with previous observations that the momentum and ion thermal transport are correlated in supershot[9] and L-mode[17] plasmas, suggesting that both are governed by a common mechanism.

IX. FLUCTUATION MEASUREMENTS

Density fluctuations have been measured with a multichannel microwave reflectometer in an ensemble of reproducible supershot plasmas with D-NBI and T-NBI at $I_p=1.6$ MA, $P_{inj} \sim 15$ MW. At $r/a \sim 0.5$, the density fluctuation level and correlation length in D plasmas are ~1% and ~1 cm, respectively. At this radius the ratio of χ_i^{tot} during D-NBI to that during T-NBI is ~1.5–1.6, and the corresponding ratio for D_e is ~1.4–1.5. As shown in Fig. 8, the fluctuation amplitude during D-NBI and T-NBI plasmas is identical within measurement uncertainty (±20%), suggesting that properties of the turbulence other than its amplitude must be responsible for the observed change in transport. The density correlation length appears to be somewhat shorter in tritium (~0.8 cm), however, an analysis is in progress to determine whether this apparent trend is greater than the measurement uncertainty. Microwave scattering measurements at $k_\theta=3.5$

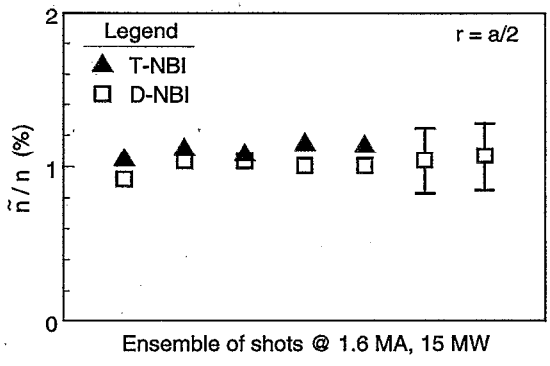

FIG. 8. Electron density fluctuation amplitude measured by correlation reflectometry in an ensemble of reproducible supershot plasmas with 15 MW of neutral–beam heating at $r/a=0.5$.

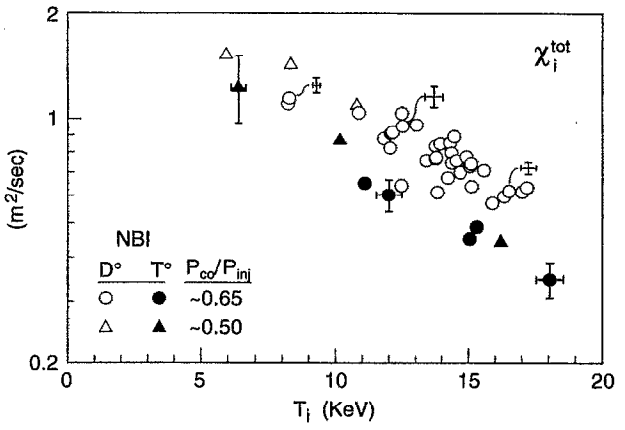

FIG. 9. Variation of χ_i^{tot} with T_i at $r/a=\frac{1}{3}$.

cm^{-1} also show no change in fluctuation amplitude, however, this measurement technique provides poorer spatial localization and has larger statistical uncertainty ($\pm 40\%$).

X. DISCUSSION

Previous studies of transport in deuterium supershots have noted a favorable correlation of χ_i^{tot} with T_i and other related parameters,[32] with χ_i varying roughly as $1/T_i$ in the plasma core. In addition, a number of microturbulence theories predict a strong dependence of the plasma transport on T_i/T_e. Such dependencies could amplify an intrinsic isotopic dependence, and make it appear to be stronger. However, as shown in Fig. 9, by comparing T-NBI plasmas with D-NBI plasmas of slightly higher P_{inj}, the isotopic variation in χ_i^{tot} at $r=a/3$ is clearly apparent at fixed local T_i. Despite the differences in P_{inj}, the cluster of T-NBI and D-NBI points near $T_i \sim 15$ keV in Fig. 9 have the same local values of n_e and L_{n_e} to better than 10%. There is no significant difference observed in either v_ϕ or ∇v_ϕ for these plasmas, suggesting that changes in $E_r \times B$ shear (which has been identified as the cause of improved confinement in the DIII-D VH mode[33]), are not responsible for reduced transport during T-NBI. The T-NBI plasmas have $\sim 10\%$ lower values of L_{T_i} and L_{T_e}, indicating slightly stronger gradients, which would be expected by ion temperature gradient turbulence models to correlate with *increased* transport. Both the T-NBI and D-NBI plasmas have $T_i/T_e = 2.9 \pm 0.1$. Thus, the strong change in χ_i^{tot} is not due to a dependence on other local thermal plasma parameters, and appears to depend only on the change in isotopic content.

There is also no evidence for significant changes in the q profile between D-NBI and T-NBI. The q profile computed by TRANSP by solving the current diffusion equation assuming neoclassical resistivity, and including beam-driven and bootstrap currents, is very similar for the D-NBI and T-NBI plasmas shown in Fig. 2; the computed shear lengths differ by only 8%–12% for $r/a=0.3-0.4$, and 2%–6% for $r/a=0.5-0.9$. The inversion radius of the first sawtooth after the termination of beam heating is the same for D-NBI and T-NBI to within ~ 2 cm, approximately the resolution of the ECE measurement. No sawteeth are observed during NBI at high power.

If the dependence on $\langle A \rangle$ is expressed at approximately constant local plasma parameters, particularly constant T_i, the relation $\chi_i^{tot} \propto \langle A \rangle^{-1.8 \pm 0.4}$ is inferred. It is interesting that, when combined with the correlation of χ_i^{tot} and $1/T_i$, this implies that roughly $\chi_i \propto A^{-1} \rho_i^{-2}$ (for fixed B), opposite to the gyro-Bohm dependence. This disagreement with the theoretical scalings is much stronger than that implied by the global scalings.

XI. SUMMARY

Confinement and local transport have been analyzed in high confinement supershot plasmas heated by either deuterium or tritium neutral beams. For strongly heated plasmas, tritium fueled plasmas have 25% higher stored energy and τ_E than comparable deuterium fueled plasmas, implying that $W_{tot} \propto \langle A \rangle^{0.85 \pm 0.20}$ for these plasmas. Of this increase in stored energy, 65%–80% is due to the thermal plasma, resulting in a thermal confinement scaling of $W_{thermal} \propto \langle A \rangle^{0.89 \pm 0.20}$. Analysis of the thermal transport indicates that most of the improvement is due to a large drop in χ_i^{tot}, and a small decrease in χ_e^{tot}. The implied isotopic mass scalings are $\chi_i^{tot} \propto \langle A \rangle^{-2.6 \pm 0.5}$ and $D_e \propto \langle A \rangle^{-1.4 \pm 0.2}$ for fixed P_{inj}. A similar decrease is observed for χ_ϕ^{tot} in plasmas with unidirectional injection. For fixed *local* plasma parameters, in particular, fixed T_i, an approximate scaling of $\chi_i^{tot} \propto \langle A \rangle^{-1.8 \pm 0.4}$ is obtained. The observed isotopic variation of χ_i^{tot} cannot be explained by a simple dependence on T_i/T_e, or by its previously observed correlation with T_i^{-1} in the supershot regime. The striking contrast in the strength of isotope scaling of χ_i^{tot} between the supershot (D/T) and L-mode (H/D) regimes may serve as a useful benchmark for proposed theoretical models of plasma transport. Finally, the strongly favorable isotope dependence of χ_i^{tot} and τ_E in D–T plasmas has very favorable implications for D–T operation in ITER and future reactors.

ACKNOWLEDGMENTS

We are grateful for the support of R. J. Hawryluk, K. McGuire, and the TFTR technical operations staffs, and for discussions with W. Dorland, L. Grisham, G. Hammett, W. Tang, and S. Zweben.

This work was supported by U.S. Department of Energy Contract No. DE-AC02-76-CHO-3073.

[1] M. Bessenrodt-Weberpals, F. Wagner, the ASDEX team, the ICRH team, the LH team, the NI team, the Pellet Injection team, the PSI group, O. Gehre, L. Giannone, J. V. Hofmann, A. Kallenbach, K. McCormick, V. Mertens, H. D. Murmann, F. Ryter, B. D. Scott, G. Siller, F. X. Soldner, A. Stabler, K.-H. Steuer, U. Stroth, N. Tsois, H. Verbeek, and H. Zohm, Nucl. Fusion **33**, 1205 (1993).

[2] P. Yushmanov, T. Takizuka, K. Riedel, O. Kardaun, J. Cordey, S. Kaye, and D. Post, Nucl. Fusion **30**, 1999 (1990).

[3] K. Thomsen, Nucl. Fusion **34**, 131 (1994).

[4] W. Dorland, M. Kotschenruether, M. A. Beer, G. W. Hammett, R. E. Waltz, R. R. Dominguez, P. M. Valanju, W. H. Miner, J. Q. Dong, W. Horton, F. L. Waelbroeck, T. Tajima, and M. J. LeBrun, "Comparison of nonlinear toroidal turbulence simulations with experiments," in *Proceedings of the 15th International Conference on Plasma Physics and Con-*

trolled Nuclear Fusion Research, Seville, 1994 (International Atomic Energy Agency, Vienna, in press), Paper No. IAEA-CN-60/D-P-I-6.
[5]G. W. Hammett, M. A. Beer, J. C. Cummings, W. Dorland, W. W. Lee, H. E. Mynick, S. E. Parker, R. A. Santoro, M. Artun, H. P. Furth, T. S. Hahm, G. Rewoldt, and W. M. Tang, "Advances in simulating tokamak turbulent transport," Paper No. IAEA-CN-60/D-2-II-1, in Ref. 4.
[6]K. M. Young, Plasma Phys. Controlled Fusion **26**, 11 (1984).
[7]M. C. Zarnstorff, S. D. Scott, C. W. Barnes, R. Bell, C. Bush, Z. Chang, D. Ernst, R. J. Fonck, L. Johnson, E. Mazzucato, R. Nazikian, S. Paul, J. Schivell, E. J. Synakowski, H. Adler, M. Bell, R. Budny, E. Fredrickson, B. Grek, A. Janos, D. Johnson, D. McCune, H. Park, A. Ramsey, M. H. Redi, G. Taylor, M. Thompson, and R. Wieland, "Heating and transport in TFTR D–T plasmas," in Ref. 4, Paper No. IAEA-CN-60/A-2-I-2.
[8]J. D. Strachan, Phys. Rev. Lett. **58**, 1004 (1987).
[9]S. Scott, P. Diamond, R. Fonck, R. Goldston, R. Howell, K. Jaehnig, G. Schilling, E. Synakowski, M. Zarnstorff, C. Bush, E. Fredrickson, K. Hill, A. Janos, D. Mansfield, D. Owens, H. Park, G. Pautasso, A. Ramsey, J. Schivell, G. Tait, W. Tang, and G. Taylor, Phys. Rev. Lett. **64**, 531 (1990).
[10]A. Kallenbach, H. M. Mayer, G. Fussman, V. Mertens, U. Stroth, and O. Vollmer, Plasma Phys. Controlled Fusion **33**, 595 (1991).
[11]B. Balet, F. Cordey, and P. Stubberfield, Plasma Phys. Controlled Fusion **34**, 3 (1992).
[12]R. J. Hawryluk, Phys. Rev. Lett. **72**, 3530 (1994).
[13]S. Scott, D. R. Ernst, M. Murakami, H. Adler, C. W. Barnes, M. G. Bell, R. Bell, R. V. Budny, C. E. Bush, Z. Chang, H. Duong, L. R. Grisham, E. D. Fredrickson, B. Grek, R. J. Hawryluk, K. W. Hill, J. Hosea, D. L. Jassby, D. W. Johnson, L. C. Johnson, M. J. Loughlin, D. K. Mansfield, K. M. McGuire, D. M. Meade, D. M. Mikkelsen, J. Murphy, H. K. Park, A. T. Ramsey, J. Schivell, C. H. Skinner, J. D. Strachan, E. J. Synakowski, G. Taylor, M. E. Thompson, R. Wieland, and M. C. Zarnstorff, Phys. Scr. **51**, 394 (1995).
[14]B. W. Stallard, D. A. Content, R. J. Groebner, D. N. Hill, R. James, J. M. Lohr, T. Luce, K. Matsuda, M. J. Mayberry, C. P. Moeller, R. Praeter, T. C. Simonen, and R. T. Snider, Nucl. Fusion **30**, 2235 (1990).
[15]F. Wagner, M. Bessenrodt-Weberpals, H. U. Fahrbach, O. Gruber, W. Herrmann, P. McCarthy, K. McCormick, H. D. Murmann, K. H. Steuer, and H. Verbeek, "Isotope dependence of Ohmic discharge parameters of Asdex," in *Proceedings of the 16th European Conference on Controlled Fusion and Plasma Heating*, Venice, 1989 (European Physical Society, Petit-Lancy, Switzerland, 1989), Part I, p. 195.
[16]R. Groebner, W. Pfeiffer, F. Blau, K. Burrell, E. Fairbanks, R. Seraydarian, H. John, and R. Stockdale, Nucl. Fusion **26**, 543 (1986).
[17]S. D. Scott, Phys. Fluids B **2**, 1300 (1990).
[18]D. P. Schissel, K. H. Burrell, J. C. DeBoo, R. J. Groebner, A. G. Kellman, N. Ohyabu, T. H. Osborne, M. Shimada, R. T. Snider, R. D. Stambaugh, and T. S. Taylor, Nucl. Fusion **29**, 185 (1989).
[19]D. Schissel, N. Brooks, K. Burrell, J. DeBoo, R. J. Groebner, G. Jackson, A. Kellman, L. Lao, M. Matsumoto, T. Osborne, R. Stambaugh, S. Wolfe, and the DIII-D Research Team, "Confinement scaling studies in DIII-D," in Ref. 15, pp. 115–118.
[20]F. Wagner, M. Bessenrodt-Weberpals, L. Giannone, A. Kallenbach, K. McCormick, F. X. Soldner, and U. Stroth, "The isotope dependence of confinement in ASDEX: Part 2, in *Proceedings of the 17th European Conference on Controlled Fusion and Plasma Heating*, Amsterdam, 1990, (European Physical Society, Petit-Lancy, Switzerland, 1990) Part I, p. 58.
[21]F. Tibone, B. Balet, M. Bures, J. G. Cordey, T. T. C. Jones, P. J. Lomas, K. Lawson, H. W. Morsi, P. Nielsen, D. F. H. Start, A. Tanga, A. Taroni, K. Thomsen, and D. J. Ward, Nucl. Fusion **33**, 1319 (1993).
[22]N. Suzuki, Y. Miura, M. Hasegawa, K. Hoshino, S. Kasai, T. Kawakami, H. Kawashima, T. Matoba, T. Matsuda, H. Matsumoto, M. Mori, K. Odajima, H. Ogawa, T. Ogawa, H. Ohtsuka, S. Senguko, T. Shoji, H. Tamai, Y. Uesugi, T. Yamamoto, T. Yamauchi, K. Hasagawa, A. Honda, I. Ishibori, Y. Kashiwa, T. Shitaba, T. Shibuya, T. Shiina, T. Tani, and K. Yokoyama, "Characteristics of the H-mode in divertor configuration on JFT-2M tokamaks," in *Proceedings of the 14th European Conference on Controlled Fusion and Plasma Heating*, Madrid, 1987, Europhysics Conference Abstracts (European Physical Society, Petit-Lancy, Switzerland, 1987), Part I, p. 217.
[23]J. Ongena, A. M. Messiaen, G. V. Wassenhove, R. R. Weynants, P. Borgermans, P. Dumortier, F. Durodié, R. Koch, P. E. Vandenplas, R. van Nieuwenhove, G. van Oost, and M. Vervier, in *Plasma Physics and Controlled Nuclear Fusion Research 1992* (International Atomic Energy Agency, Vienna, 1993), Vol. 1, pp. 725–731.
[24]C. H. Skinner, D. P. Stotler, R. V. Budny, H. Adler, and A. T. Ramsey, Rev. Sci. Instrum. **66**, 646 (1995).
[25]H. Towner, R. Goldston, G. Hammett, J. Murphy, C. Phillips, S. Scott, M. Zarnstorff, and D. Smithe, Rev. Sci. Instrum. **63**, 4753 (1992).
[26]R. J. Hawryluk, in *Physics of Plasmas Close to Thermonuclear Conditions* (Commission of the European Communities, Brussels, 1980), Vol. 1, p. 19.
[27]R. B. Howell, R. J. Fonck, R. J. Knize, and K. P. Jaehnig, Rev. Sci. Instrum. **59**, 1521 (1988).
[28]M. von Hellerman, W. Mandl, H. P. Summers, H. Weisen, A. Boileau, P. D. Morgan, H. Morsi, R. Konig, M. F. Stamp, and R. C. Wolf, Rev. Sci. Instrum. **61**, 3479 (1990).
[29]R. K. Janev, Atom. Data Nucl. Data Tables **55**, 201 (1993).
[30]M. C. Zarnstorff, in *Plasma Physics and Controlled Nuclear Fusion Research*, Nice 1988 (International Atomic Energy Agency, Vienna, 1989), Vol. 1, p. 183.
[31]P. C. Efthimion, L. C. Johnson, C. H. Skinner, J. D. Strachan, E. J. Synakowski, M. Zarnstorff, H. Adler, C. B. Barnes, R. Bell, R. V. Budny, R. J. Fonck, F. C. Jobes, J. Kampershroer, S. E. Kruger, W. W. Lee, M. Laughlin, D. McCune, G. McKee, D. R. Mikkelsen, D. Mueller, D. K. Owens, A. T. Ramsey, G. Rewoldt, A. L. Roquemore, D. P. Stotler, B. C. Stratton, W. M. Tang, G. Taylor, and the TFTR group, "Tritium transport, influx, and helium ash measurements on TFTR during DT operation," in Ref. 4, Paper No. IAEA-CN-60/A-2-II-6.
[32]D. M. Meade, in *Plasma Physics and Controlled Nuclear Fusion Research*, Washington DC, 1990 (International Atomic Energy Agency, Vienna, 1991), Vol. 1, pp. 9–24.
[33]K. H. Burrell, M. E. Austin, T. N. Carlstrom, S. Coda, E. J. Doyle, P. Gohil, R. J. Groebner, J. Kim, R. J. L. Haye, L. L. Loa, J. Lohr, R. A. Moyer, T. H. Osborne, W. A. Pebbles, C. L. Rettig, T. L. Rhodes, and D. M. Thomas, "H-mode and VH-mode confinement improvement in DIII-D: Investigations of turbulence, local transport and active control of the shear in the $E\times B$ flow," in Ref. 4.